Periodica Polytechnica Electrical Engineering and Computer Science

Compact MIMO Vivaldi Tapered Slot Antenna for UWB Systems with WLAN/WiMax Band-notched Features

Mokhtar Mokhtari[1,2*], Mouloud Challal[3], Ali Mansoul[2], Rachid Oussaid[1]

[1] Laboratory of Instrumentation, Faculty of Electrical Engineering, University of Sciences and Technology Houari Boumediene, P.O.B. 32, 16111 Bab Ezzouar, Algeria
[2] Center for Development of Advanced Technologies, Cité 20 août 1956,16081 Baba Hassen, Algeria
[3] Signals and Systems Laboratory, Institute of Electrical and Electronic Engineering, University M'Hamed BOUGARA of Boumerdes, 35000 Boumerdes, Algeria
[*] Corresponding author, e-mail: m.mokhtari@usthb.dz

Received: 05 May 2026, Accepted: 03 August 2026, Published online: 17 September 2026

Abstract

This manuscript presents a compact Multiple-Input Multiple-Output (MIMO) Ultra-Wideband (UWB) Vivaldi tapered slot antenna with dual band-notched characteristics. The proposed antenna has overall dimensions of 20 × 29.4 mm^2, and its design procedure and performance are comprehensively investigated. A detailed description of the antenna design evolution is provided. A stepped feed line is employed to enhance the impedance bandwidth for a reflection coefficient below -10 dB, while a meandered slot and an arc-shaped stub are incorporated to create notched bands at the WiMAX and WLAN frequencies, respectively. To improve the isolation between the MIMO antenna elements, a tuning fork-shaped slot is etched in the ground plane between the two ports. The measured results demonstrate that the proposed antenna operates over a wide bandwidth from 2.6 to 12 GHz, while effectively rejecting the 3.5 GHz and 5.6 GHz bands, corresponding to the WiMAX and WLAN bands, respectively. In addition, a minimum isolation of 18 dB is achieved across the operating band. Owing to its compact size, good MIMO diversity performance, and dual band-notched characteristics, the proposed antenna is a promising candidate for modern wireless communication systems and UWB applications.

Keywords

MIMO, UWB, band-notched, Vivaldi

1 Introduction

Multiple-input multiple-output (MIMO) antennas have emerged as a promising technology for modern wireless communication systems due to their ability to enhance channel capacity, improve link reliability, increase data throughput, and extend communication coverage [1]. In particular, Ultra-Wideband (UWB) MIMO antennas play a vital role in microwave communication and imaging systems by providing high data transmission rates, improved detection accuracy, and enhanced microwave imaging capabilities [2]. The UWB frequency band allocated by the Federal Communications Commission (FCC), ranging from 3.1 GHz to 10.6 GHz [3], enables these antennas to support a broad range of wireless applications.

Over the past decades, considerable research has been devoted to the development of compact UWB antennas with wide impedance bandwidths. However, the coexistence of UWB systems with other wireless communication services, such as Worldwide Interoperability for Microwave Access (WiMAX), Wireless Local Area Networks (WLAN), and X-band satellite communication, introduces electromagnetic (EM) interference within the UWB operating band. To mitigate this issue, incorporating band-notched characteristics into UWB antenna designs has become an effective and widely adopted approach, enabling the selective rejection of interfering frequency bands while preserving the desired ultra-wideband performance [4].

Numerous UWB MIMO antenna designs have been reported in the literature, employing various isolation enhancement techniques. These techniques include element separation [5, 6], the use of stubs [7, 8], Electromagnetic Band Gap (EBG) structures [9], fork-shaped Defected Ground Structure (DGS) configurations [10], fence-type DGS techniques [1], neutralization lines [11], and polarization diversity approaches [12, 13]. Each of these methods

Cite this article as: Mokhtari, M., Challal, M., Mansoul, A., Oussaid, R. "Compact MIMO Vivaldi Tapered Slot Antenna for UWB Systems with WLAN/WiMax Band-notched Features", Periodica Polytechnica Electrical Engineering and Computer Science, 2026. https://doi.org/10.3311/PPee.44580

provides an effective solution for reducing mutual coupling and improving the isolation between antenna elements.

Despite significant advancements in UWB MIMO antenna design, antenna size remains a major challenge for designers. The compact arrangement of multiple antenna elements in MIMO systems often leads to strong mutual coupling, which can negatively affect diversity performance. Therefore, achieving compact size while effectively addressing high mutual coupling remains a crucial challenge in MIMO antenna design [14]. Furthermore, MIMO systems utilizing the UWB spectrum may face challenges due to electromagnetic interference with other communication standards. To mitigate this issue, various notch techniques have been adopted for the design of band-rejected MIMO antennas. Noteworthy examples include a two-element UWB antenna with a WLAN band notch [15]. Every antenna element has a rectangular stepped-slot, serving as the primary radiator, and a z-shaped slot for rejecting the WLAN band. An inverted T-shaped slot is introduced to enhance isolation. In [16], the UWB MIMO Vivaldi antenna exhibits WLAN and C-band band-notched characteristics, achieving band rejections through the use of varying in size Split Ring Resonators (SRRs), and the mutual coupling is reduced using a T-shaped slot. In [17], a MIMO UWB antenna with two-band notched characteristics at 5G and Wi-Fi 6E applications is presented, accomplished by etching a Complementary Split Ring Resonator (CSRR) and inserting an SRR. Isolation is achieved using a three-line stub between láthe two radiating elements. In [4], a four-port MIMO antenna with three notched bands at WLAN, X-band, and WiMAX is proposed, featuring etched C-shaped slots and an L-shaped slot. The isolation is improved by the orthogonal orientation of antenna elements and the insertion of a cross-shaped decoupling structure. These innovative techniques aim to enhance coexistence with other wireless systems and increase the overall capability of UWB MIMO antenna systems.

Although numerous UWB MIMO antennas with band-notched characteristics have been reported, most existing designs either have relatively large dimensions, rely on complex decoupling structures or multiple resonant elements to achieve band rejection, or provide only a single notched band. Consequently, designing a compact UWB MIMO Vivaldi antenna that simultaneously offers dual band-notched characteristics, high isolation, structural simplicity, and excellent diversity performance remains a significant challenge.

To address these limitations, this paper proposes a compact UWB MIMO Vivaldi tapered slot antenna with dual band-notched characteristics. The WiMAX and WLAN band rejections are independently realized by incorporating a meandered slot and an arc-shaped stub, respectively. Furthermore, a compact tuning fork-shaped slot etched in the ground plane is introduced to effectively reduce mutual coupling while preserving the antenna's ultra-wide impedance bandwidth. The proposed design achieves an excellent balance between compact size, filtering capability, MIMO performance, and structural simplicity. In addition, the band-notching mechanism is thoroughly analyzed through parametric studies and surface current distributions. Experimental results are in good agreement with the simulated results, thereby validating the effectiveness of the proposed antenna design.

2 Antenna design and study

2.1 Antenna structures

The proposed antenna is printed on an FR-4 substrate with a thickness of 1.6 mm, a relative dielectric constant of 4.3, and a loss tangent of 0.02. The overall dimensions of the antenna are 20 × 29.4 mm^2. Two stepped microstrip feed lines are printed on the top layer, while the bottom layer incorporates a Vivaldi tapered slot, a meandered slot, an arc-shaped stub, and a decoupling structure. The configuration of the proposed antenna is illustrated in Fig. 1, and the optimized dimensions obtained using CST Microwave Studio are listed as follows: W_s = 29.4 mm, W_1 = 2 mm, W_2 = 0.6 mm, W_3 = 2.9 mm, W_m = 9.8 mm, Ls = 20 mm, L_1 = 6 mm, L_2 = 4 mm, L3 = 4 mm, L_m = 1.4 mm, L_i = 7.3 mm, R_i = 1.35 mm, H_1 = 0.55 mm, H_2 = 8.6 mm, S_m = 0.5 mm, La = 8.1 mm. The main radiator of the antenna consists of an exponential tapered slot etched into the ground plane. The mathematical expression defining the exponential taper profile is given as Eq. (1)–(3):

$$y = C_1 e^{rx} + C_2 , \tag{1}$$

where

$$C_1 = \frac{y_2 - y_1}{e^{rx_2} - e^{rx_1}} , \tag{2}$$

$$C_2 = \frac{y_1 e^{rx_2} - y_2 e^{rx_1}}{e^{rx_2} - e^{rx_1}} . \tag{3}$$

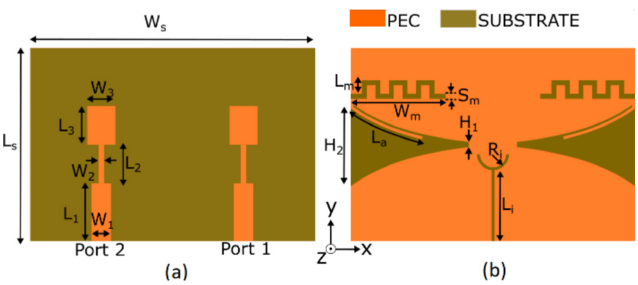

Fig. 1 Layout of the proposed antenna: (a) Top view; (b) Bottom view

The taper profile is defined by the opening rate (r = 0.15) and determined by the bottom point and peak point: P_1 (x_1, y_1) and P_2 (x_2, y_2), respectively; and can be determined by H_2 and H_1.

2.2 Antenna design evolution

First, we start our design with a single antenna element fed by a standard 50 Ω microstrip line as depicted in Fig. 2 (step 1), to improve the impedance matching, a stepped microstrip feed line is used (step 2). The WiMax band rejection is achieved by etching from the ground plane a meandered slot positioned above the tapered slot, and to reject the WLAN band an arc-shaped stub is connected to the top flare of the Vivaldi antenna as shown in Fig. 2 (step 3, and step 4, respectively). By placing two elements next to each other a mutual coupling is created between the two ports (step 5), to cancel it an isolation structure comprising a tuning fork-shaped slot is inserted between the two elements (step 6). This configuration reduces the surface current density, as well as mutual coupling between the two elements.

According to Fig. 3, the operational bandwidth of the UWB single antenna element, using a stepped feed line, ranges from 3.5 GHz to 12 GHz. With the inclusion of the meandered slot, the antenna operates within the frequency range of 2.9 GHz to 12 GHz, featuring a band rejection at 3.5 GHz [3.2–4 GHz]. Additionally, the insertion of the arc-shaped stub enables the antenna to reject a second band at 5.5 GHz [4.9–6 GHz]. Moreover, by incorporating an isolation structure between the two elements, the maximum mutual coupling is significantly reduced from −7 dB to −15.4 dB. as shown in Fig. 4. The final UWB MIMO antenna design, incorporating all modifications, achieves an operational bandwidth from 2.9 GHz to 12 GHz, with notches at 3.5 GHz and 5.5 GHz, and an isolation exceeding 15.4 dB.

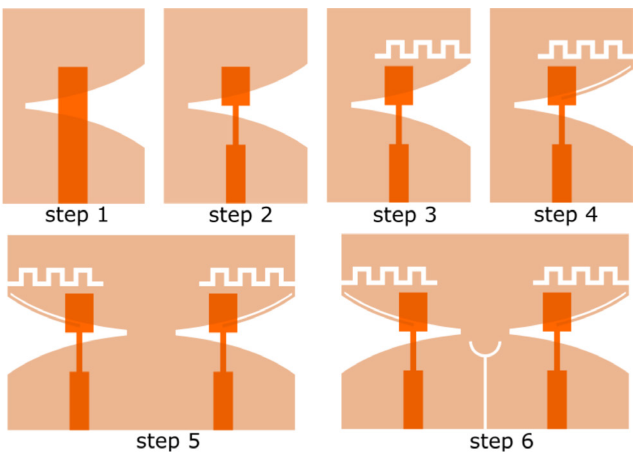

Fig. 2 Design evolution of the suggested antenna

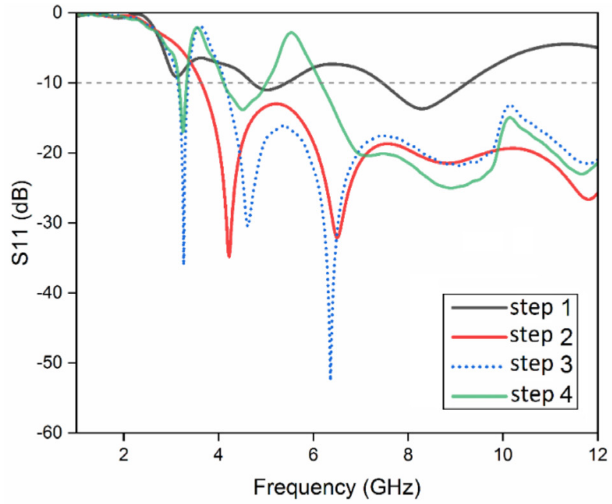

Fig. 3 Reflection coefficient of single antenna element design evolution

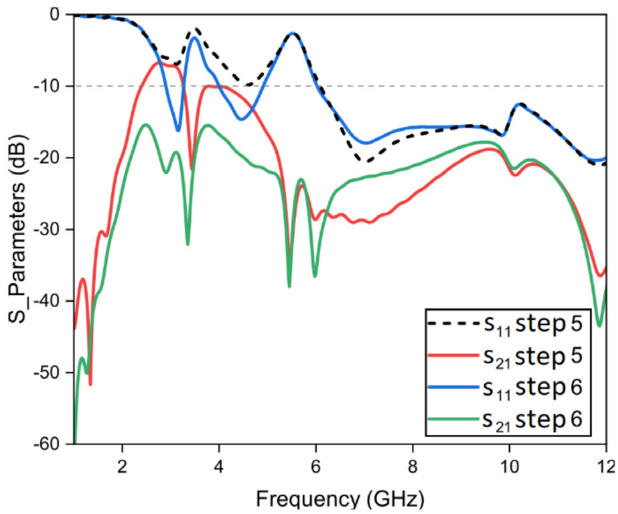

Fig. 4 *S*-Parameters of the MIMO antenna design

To demonstrate the impact of the insertion of the isolation structure on reducing mutual coupling within the antenna, a study of current distribution was conducted on the structure with and without the isolation mechanism. The study was performed at a frequency of 3.1 GHz, with port 1 excited and port 2 terminated by a 50 Ω load (Fig. 5). Simulation results show a significant reduction in current density around the second port of the antenna

2.3 Filtering technique

Parametric studies on the length of the meandered slot and the arc-shaped stub are shown in Fig. 6 and Fig. 7, respectively. It is seen that altering the length of the meandered slot modifies the first notched band (WiMAX band) while leaving the second unchanged. Similarly, adjusting the length of the arc-shaped stub modifies the second notched band (WLAN band) without affecting the first. It is noteworthy that elongating both the slot and the stub leads to a

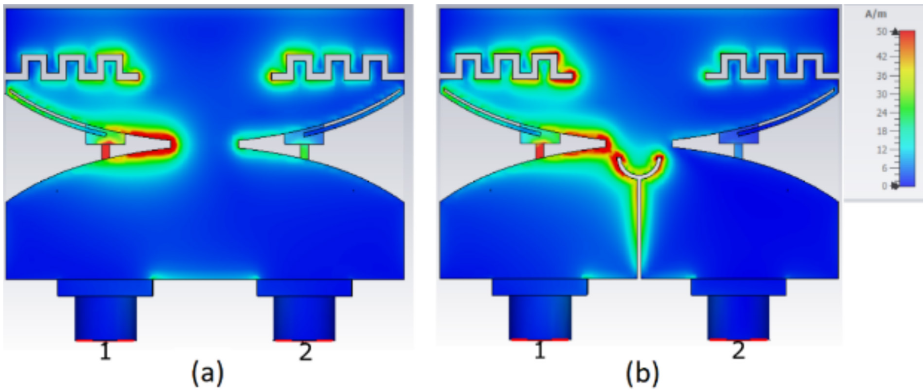

Fig. 5 Distribution of surface current at 3.1 GHz: (a) without isolation structure; (b) with isolation structure

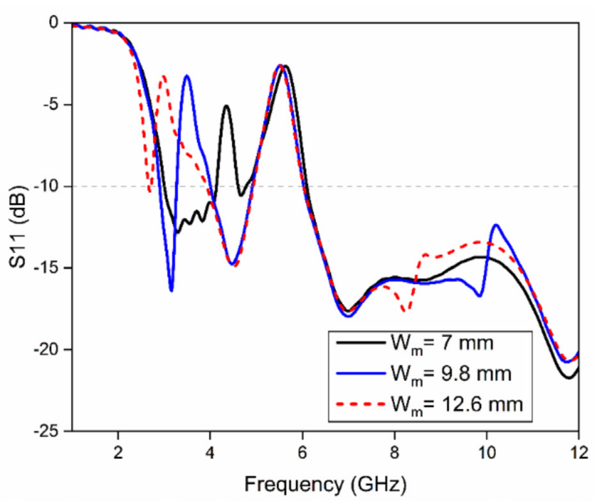

Fig. 6 S_{11} response for different W_m values

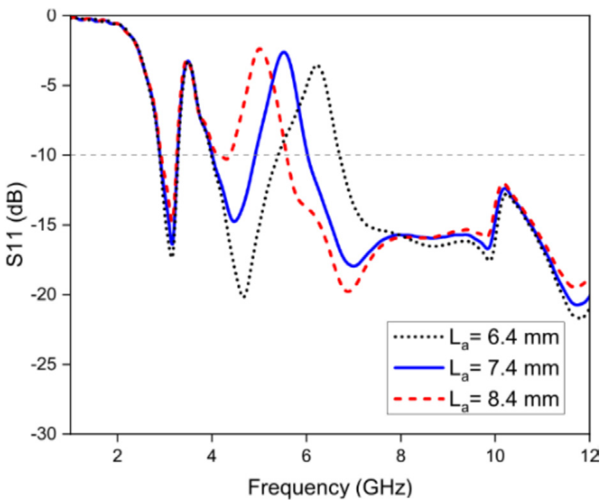

Fig. 7 S_{11} response for different L_a values

reduction in the central frequency of the respective band-notches and *vice versa*.

According to [18] the meandered slot acts as parallel inductance capacitance (*LC*) circuit, and the central frequency of the band notch can be estimated using Eqs. (4–5):

$$F_{\text{notch1}} \approx \frac{C}{4L_{\text{slot}}\sqrt{\frac{\varepsilon_r + 1}{2}}}, \quad (4)$$

$$L_{\text{slot}} = W_m + 3L_m, \quad (5)$$

where C is the speed of the light, ε_r relative permittivity, and L_{slot} is the total length of the meandered slot and is approximately quarter guided wavelength ($\lambda_g/4$) at 3.5 GHz.

For the arc-shaped stub the relationship between the central frequency of the notched band and the length of the stub can be represented as Eq. (6):

$$F_{\text{notch2}} \approx \frac{C}{4L_a\sqrt{\frac{\varepsilon_r + 1}{2}}}, \quad (6)$$

where L_a is the length of the arc-shaped stub which is near to $\lambda_g/4$ at 5 .5 GHz

The surface current distributions of the designed antenna at the two rejected frequencies, with Port 1 excited and Port 2 terminated with a 50 Ω load, are illustrated in Fig. 8. At 3.5 GHz, the current is mainly concentrated around the meandered slot, whereas at 5.5 GHz, the current density is predominantly distributed along the arc-shaped stub. These observations confirm that the meandered slot is responsible for generating the WiMAX band rejection, while the arc-shaped stub contributes to the WLAN band rejection.

2.4 Fabrication and discussion

The photograph of the realized MIMO antenna is displayed in Fig. 9, Measurements were carried out using a KEYSIGHT PNA N5224A network analyzer, and Fig. 10 illustrates a graphic comparison of the measured and simulated *S*-parameters. The measured operating bandwidth spans from 2.6 to 12 GHz, with a band notch at 3.5 GHz [3.1–3.9 GHz], and at 5.6 GHz [5–5.9 GHz]. The isolation is below 18 dB across the entire operating bandwidth, and

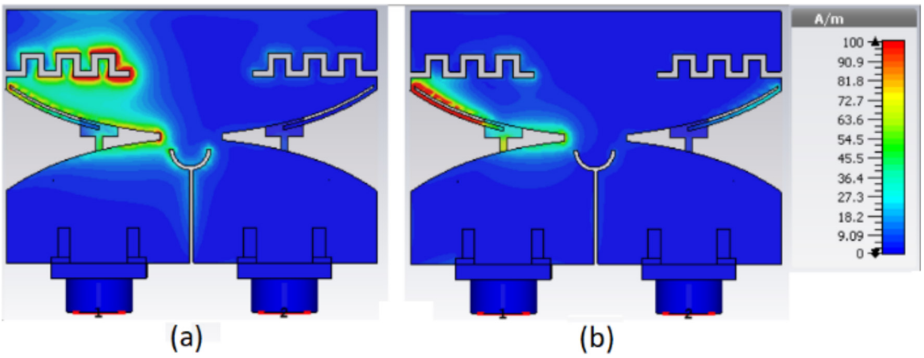

Fig. 8 Distribution of surface current at: (a) 3.5 GHz; (b) 5.5 GHz

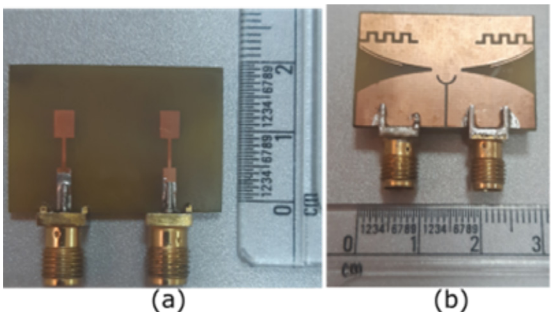

Fig. 9 Fabricated prototype: (a) Top view; (b) Bottom view

there is a significant correlation between the simulated and measured results.

Fig. 11 illustrates the normalized radiation patterns of the proposed MIMO antenna at various frequencies in both the XOY-plane (E-plane) and the XOZ-plane (H-plane). The radiation patterns are obtained by exciting Port 1 while terminating Port 2 with a 50 Ω load. It can be observed that the antenna exhibits a directive radiation pattern in both planes across the operating frequency range. The variations of the realized gain and radiation efficiency with frequency are illustrated in Fig. 12. As expected, both parameters exhibit a significant reduction at the notched WiMAX and WLAN frequency bands, confirming the effectiveness of the proposed band-rejection mechanism. Outside the rejected bands, the antenna achieves a maximum realized gain of 5.3 dBi at 9 GHz and a peak radiation efficiency of 90.5% at 8 GHz, demonstrating its suitability for UWB wireless communication applications.

The envelope correlation coefficient (*ECC*) is an essential metric to consider during the design of a MIMO antenna, where the optimum level of *ECC* should be equal to or less than 0.3, the relationship between *ECC* and *S*-parameters is described as Eq. (7)[12]:

$$ECC = \frac{\left|S_{11}^{*}S_{12} + S_{21}^{*}S_{22}\right|^{2}}{\left(1-\left|S_{11}\right|^{2}-\left|S_{21}\right|^{2}\right)\left(1-\left|S_{22}\right|^{2}-\left|S_{12}\right|^{2}\right)} . \quad (7)$$

The diversity gain (*DG*), which is closely related to the envelope correlation coefficient (*ECC*), is another important parameter for evaluating the diversity performance of MIMO antennas. It is calculated using Eq. (8):

$$DG = 10\sqrt{1-ECC^{2}} . \quad (8)$$

Fig. 13 presents the calculated *ECC* and *DG* values, demonstrating low *ECC* levels (*ECC* < 0.07) across the entire operating bandwidth. The *DG* remains approximately 10 dB throughout the operating band, except at the rejected frequency bands, where it slightly decreases

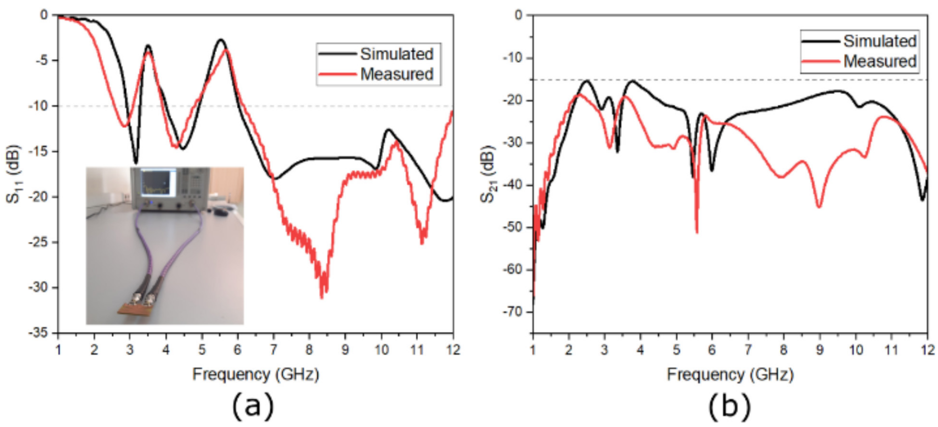

Fig. 10 Magnitude of *S*-parameters: (a) Reflection coefficient; (b) Isolation

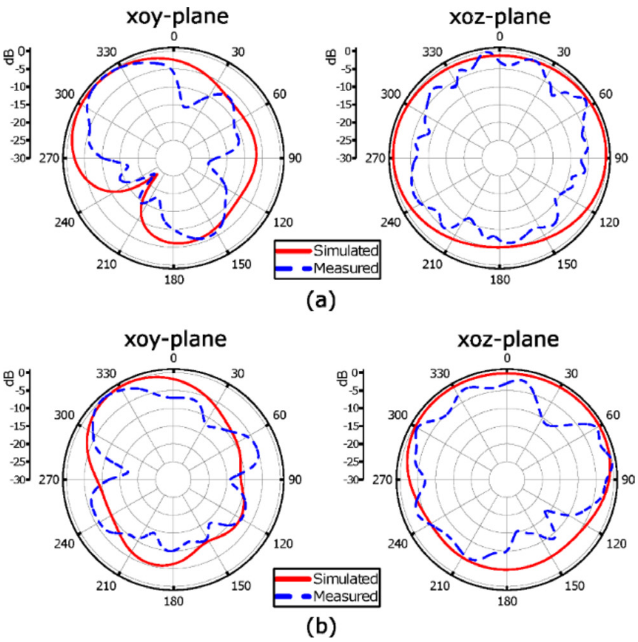

Fig. 11 Normalized radiation patterns at: (a) 4.5 GHz; (b) 7 GHz

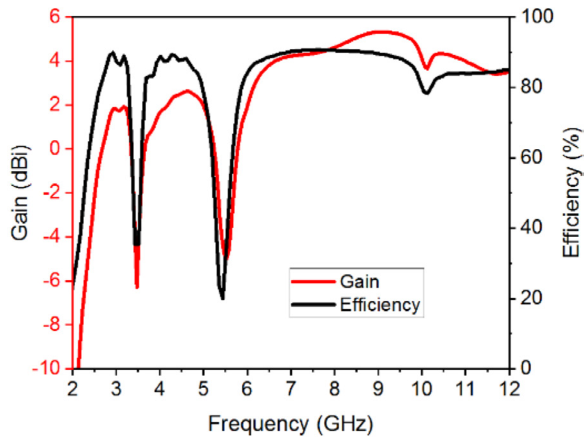

Fig. 12 Realized gain and efficiency over frequency range

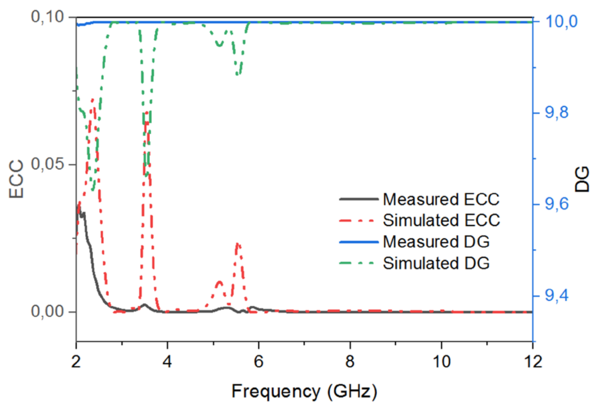

Fig. 13 *ECC* and *DG* of the proposed MIMO antenna

to 9.6 dB. These results confirm that the proposed antenna exhibits excellent diversity performance and is suitable for MIMO applications.

The channel capacity loss (*CCL*) is another important parameter for evaluating the performance of MIMO antenna systems, as it quantifies the reduction in channel capacity resulting from mutual coupling and signal correlation between antenna elements. For efficient MIMO operation, the *CCL* should remain below 0.4 bits/s/Hz over the operating bandwidth [12]. As illustrated in Fig. 14, the proposed antenna maintains *CCL* values well below this acceptable limit across the entire operating band, with only slight variations observed at the notched frequencies.

A comparative study of the proposed antenna in terms of size, impedance bandwidth, rejected bands, and isolation level with other recent works reported in the literature is presented in Table 1. The comparison highlights the advantages of the proposed design in achieving a compact size while maintaining wideband operation, dual band-notched characteristics, and good isolation performance.

3 Conclusion

In this work, a compact UWB MIMO Vivaldi tapered slot antenna with dual band-notched characteristics is presented. The antenna design evolution is described, demonstrating the effective rejection of the WiMAX and WLAN bands through the incorporation of a meandered slot and an arc-shaped stub, respectively. Furthermore, the integration of a tuning fork-shaped slot improves the isolation between the antenna elements, achieving a minimum isolation level of 18 dB. A parametric study is conducted to investigate the influence of the dimensions of the structures responsible for generating the notched bands. Moreover, the filtering mechanism is thoroughly analyzed and explained. The fabricated antenna exhibits a compact size of 20 × 29.4 mm^2 and achieves an experimental operating bandwidth from 2.6 to 12 GHz, with

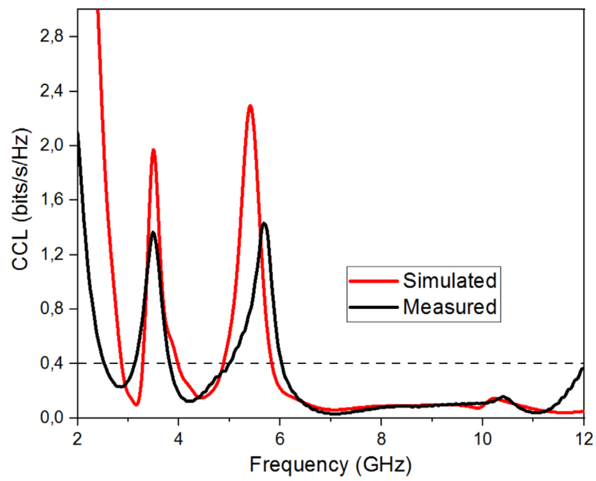

Fig. 14 CCL of the proposed MIMO antenna

Table 1 Comparison of the proposed antenna with other reported works

Ref	[4]	[5]	[6]	[8]	[15]	[16]	[17]	This work
Size (mm^2)	35.9 × 35.9	40 × 21	85 × 170	58 × 36	23 × 26	26 × 26	40 × 30	20 × 29.4
Bandwidth (GHz)	[3.2–10.8]	[2.94–11.6]	[3–12]	[2.6–27.2]	[3.1–10.6]	[2.9–11.6]	[3.05–11.6]	[2.6–12]
Bandnotched (GHz)	[3.4–3.8] [5.2–6.4] [7.1–8.8]	[3.63–4.15]	[4.93–6.47]	[2.7–4] [8.5–12]	[5.1–5.9]	[5.3–5.8] [7.85–8.55]	[3.4–3.9] [5.7–6.2]	[3.1–3.9] [5-5.9]
Filtering technique	C-shaped and L-shaped slots	U-shaped slot	Four U-shaped slot	H-shape and double C-shaped slots	Z-shaped slot	SRR	CSRR and SRR	Meandered slot and arc-shaped stub
Peak gain (dBi)	5.1	4.21	7.18	4	4.5	>6	/	5.3
efficiency (%)	93	86	/	95	92	/	67	90.5
ECC	<0.49	<0.002	<0.001	<0.01	<0.01	<0.02	<0.02	<0.07
DG	/	9.999	9.998	0.94	/	/	9.75	9.6
CCL (bits/s/Hz)	/	<0.1	<0.14	<0.4	/	/	<0.4	<0.4
Isolation (dB)	>20	>18	>25	>16	>20	>16	>15	>18

effective rejection at 3.5 GHz and 5.6 GHz. The *ECC* remains below 0.07 over the operating bandwidth, confirming the excellent diversity performance of the proposed antenna for MIMO applications. Therefore, the proposed prototype represents a promising candidate for UWB MIMO wireless communication systems.

References

[1] Wang, L., Du, Z., Yang, H., Ma, R., Zhao, Y., Cui, X., Xi, X. "Compact UWB MIMO Antenna With High Isolation Using Fence-Type Decoupling Structure", IEEE Antennas and Wireless Propagation Letters, 18(8), pp. 1641–1645, 2019. https://doi.org/10.1109/LAWP.2019.2925857

[2] Ziani, D., Meriah, S. M., Derraz, F., Merad, L. "A compact asymmetrically slotted antipodal Vivaldi antenna for MIMO imaging systems", Telecommunication Systems, 83(3), pp. 267–275, 2023. https://doi.org/10.1007/s11235-023-01013-5

[3] Breed, G. "A Summary of FCC Rules for Ultra Wideband Communications", High Frequency Electronics, 4(1), pp. 42–44, 2005.

[4] Jayant, S., Srivastava, G. "Close-Packed Quad-Element Triple-Band-Notched UWB MIMO Antenna With Upgrading Capability", IEEE Transactions on Antennas and Propagation, 71(1), pp. 353–360, 2023. https://doi.org/10.1109/TAP.2022.3222768

[5] Devana, V. N. K. R., Beno, A., Devadoss, C. P., Sukanya, Y., Ravi Sankar, Ch. V., Balamuralikrishna, P., Chandrasekhar, S., Babu, K. V. "A Compact Self Isolated MIMO UWB Antenna with Band Notched Characteristics", IETE Journal of Research, 70(8), pp. 6677–6688, 2024. https://doi.org/10.1080/03772063.2024.2310124

[6] Ahmed, B. T., Sánchez, A. M. "Vivaldi MIMO Antennas", Wireless Personal Communications, 132(1), pp. 279–304, 2023. https://doi.org/10.1007/s11277-023-10611-0

[7] Dhananjeyan, R., Ramesh, S., Kumar, D. R., Kumar, O. P. "Compact octagonal MIMO antenna system for broadband applications with enhanced isolation and wideband performance", Scientific Reports, 15(1), 18921, 2025. https://doi.org/10.1038/s41598-025-03494-7

[8] Agrawal, S., Parihar, M. S. "The Design and Investigation of a Super Wideband Antenna with Dual-Band Notch Characteristics for MIMO Application", IETE Technical Review, 41(3), pp. 366–376, 2024. https://doi.org/10.1080/02564602.2023.2255553

[9] Alnaiemy, Y., Elwi, T. A., Nagy, L. "Mutual Coupling Reduction in Patch Antenna Array Based on EBG Structure for MIMO Applications", Periodica Polytechnica Electrical Engineering and Computer Science, 63(4), pp. 332–342, 2019. https://doi.org/10.3311/PPee.14379

[10] Wang, E., Wang, W., Tan, X., Wu, Y., Gao, J., Liu, Y. "A UWB MIMO slot antenna using defected ground structures for high isolation", International Journal of RF and Microwave Computer-Aided Engineering, 30(5), e22155, 2020. https://doi.org/10.1002/mmce.22155

[11] Pandey, R., Biswas, A. K., Chakraborty, U., Roy, A. "Neutralization Line Loaded Dual Port Wideband MIMO Antenna with Enhanced Isolation Implemented on Colored Resin Fiber Material", Wireless Personal Communications, 146(2), pp. 789–816, 2026. https://doi.org/10.1007/s11277-025-11904-2

[12] Hasan, M. N., Chu, S., Bashir, S. "A DGS monopole antenna loaded with U-shape stub for UWB MIMO applications", Microwave and Optical Technology Letters, 61(9), pp. 2141–2149, 2019. https://doi.org/10.1002/mop.31877

[13] Tan, M. T., Li, X., Wei, W. H., Tan, W. X., Zhou, B., Li, J. Q. "A planar miniaturized UWB dual-polarization multiple-input-multiple-output slot antenna", Microwave and Optical Technology Letters, 62(1), pp. 432–438, 2020. https://doi.org/10.1002/mop.32032

[14] Parchin, N. O., Al-Yasir, Y. I. A., Ali, A. H., Elfergani, I., Noras, J. M., Rodriguez, J., Abd-Alhameed, R. A. "Eight-element dual-polarized MIMO slot antenna system for 5G smartphone applications", IEEE Access, 7, pp. 15612–15622, 2019. https://doi.org/10.1109/ACCESS.2019.2893112

[15] Chattha, H. T., Latif, F., Tahir, F. A., Khan, M. U., Yang, X. "Small-Sized UWB MIMO Antenna With Band Rejection Capability", IEEE Access, 7, pp. 121816–121824, 2019. https://doi.org/10.1109/ACCESS.2019.2937322

[16] Li, Z., Yin, C., Zhu, X. "Compact UWB MIMO Vivaldi Antenna With Dual Band-Notched Characteristics", IEEE Access, 7, pp. 38696–38701, 2019. https://doi.org/10.1109/ACCESS.2019.2906338

[17] Bakali, H. E. O. E., Zakriti, A., Farkhsi, A., Dkiouak, A., El Ouahabi, M. "Design and realization of dual band notch UWB MIMO antenna in 5G and Wi-Fi 6E by using hybrid technique", Progress in Electromagnetics Research C, 116, pp. 1–12, 2021. https://doi.org/10.2528/PIERC21080701

[18] ur Rehman, S., Alkanhal, M. A. S. "Design and System Characterization of Ultra-Wideband Antennas With Multiple Band-Rejection", IEEE Access, 5, pp. 17988–17996, 2017. https://doi.org/10.1109/ACCESS.2017.2715881